SonarBeat: Sonar Phase for Breathing Beat Monitoring with Smartphones

Xuyu Wang, Runze Huang, and Shiwen Mao
Department of Electrical and Computer Engineering, Auburn University, Auburn, AL 36849-5201, USA
Email: {xzw0029, rzh0038}@auburn.edu, smao@ieee.org

***Abstract*—Vital sign (e.g., breathing rate) monitoring has become increasingly more important because it can offer useful clues to medical conditions such as sleep disorders or anomalies. There is a compelling need for technologies that enable contact-free, easy deployment, and long-term vital sign monitoring for healthcare. In this paper, we present a SonarBeat system to leverage a phase based active sonar to monitor breathing rates with smartphones. We design and implement the SonarBeat system, with components including signal generation, data extraction, received signal preprocessing, and breathing rate estimation, with Andriod smartphones. Our experimental results validate the superior performance of SonarBeat in different indoor environment settings.**

***Index Terms*—Breathing monitoring; Channel State Information (CSI); Health sensing; Sonar; CSI Phase.**

I. Introduction

With the rapid development of mobile techniques and improvements in the living standard, people are paying increasingly more attention on healthcare problems and the related cost [1], [2]. It is reported that three-fourths of the total US healthcare cost are spent on treating chronic health conditions such as heart diseases, lung disorders, and diabetes [3]. Breathing signals are useful for physical health monitoring since such vital signs can offer important information for health problems, such as sudden infant death syndrome (SIDS) of sleeping infants [4]. Traditional systems require a person to wear special devices, such as a pulse oximeter [5] or a capnometer [6], which are inconvenient and uncomfortable, especially for the elders and infants. There is a compelling need for technologies that can enable contact-free, easy deployment, and long-term vital sign monitoring for healthcare.

Existing vital signal monitoring systems mainly focus on radio frequency (RF) based techniques, which utilize RF signals to capture breathing and heart movements. Existing RF based schemes include radar based and WiFi based vital sign monitoring. In the radar based category, the Doppler radar [7], [8] and the ultra-wideband radar [9] are used to estimate breathing beats, where customized hardware is used operating on a high frequency band. Moreover, Vital-Radio employs a frequency modulated continuous wave (FMCW) radar to estimate breathing and heart rates [10] with a specially designed hardware operating on a large bandwidth from 5.46 GHz to 7.25 GHz. In the WiFi based category, UbiBreathe monitors breathing signals by analyzing the received signal strength (RSS) of WiFi signals, which represents coarse channel information [11]. Another technique, mmVital [12], uses 60 GHz millimeter wave (mmWave) signals for breathing and heart rates estimation while using a larger bandwidth of about 7 GHz and high gain directional antennas at the transmitter and receiver. Recently, the authors in [13] exploit the amplitudes of WiFi CSI data to track vital signs of a sleeping person. Our recent work PhaseBeat [1] and TensorBeat [2] use the CSI phase difference data instead, for monitoring breathing and heartbeat for a single person and breathing for multiple persons. Although RF based techniques can effectively monitor vital signs over a long distance for healthcare, RF based signals can be easily influenced by environment changes such as movements of other persons in the vicinity, and are thus not suitable for certain deployment scenarios.

To this end, the smartphones can be exploited for vial sign measurement with the built in accelerometer, gyroscope [14] and microphone [15]. Usually, the smartphone needs to be placed near the body, or the person needs to wear special types of sensors that connect to the smartphone. Note that for device-free and contact-free monitoring of vital signs, attached sensors should not be used. In a recent work [16], the authors propose to use the active sonar in the smartphone by leveraging the FMCW technique for breathing monitoring. However, the FMCW based technique requires an accurate estimation of the distance between the smartphone and the chest of the person, before it can monitor the respiration of the person. When the body suddenly moves (e.g., rolling over in bed), the system needs to detect the new smartphone-chest distance, thus leading to an additional time complexity. In addition, the LLAP system employs a continuous-wave (CW) radar to measure distance and achieves device-free hand tracking using the sonar phase information [17].

Motivated by these interesting studies, we employ the sonar phase data with a smartphone to monitor the periodic signal caused by the rises and falls of the chest (i.e., inhaling and exhaling). We find that the sonar phase information can track the periodic signal of breathing beats with a high accuracy. Compared with other existing systems such as Doppler shift and FMCW [16], the sonar phase based scheme has a lower latency and complexity. In addition, the sonar phase data is highly robust to different orientations, different distances, and different breathing rates of different persons.

We first present a rigorous sonar phase analysis, and prove that the sonar phase information can capture the breathing beats with the same frequency. Built upon the sonar phase analysis, we design SonarBeat, a robust breathing monitor-

978-1-5090-2991-4/17/$31.00 ©2017 IEEE

ing system by using active sonar phase information with smartphones. The SonarBeat system consists of four modules implemented in the smartphone, including signal generation, data extraction, received signal preprocessing, and breathing rate estimation. First, it transmits an inaudible sound signal in the frequency range of 18-22 kHz by utilizing the smartphone speaker as a CW radar. Then, the signal is reflected by the chest of the person and is then received by the microphone of the same smartphone. The received signal is then processed and the breathing signal will be recovered. We implement SonarBeat with two different smartphones and validate its performance with extensive experiments that involve five persons over a period of three months in three different environments, including an office scenario, a bedroom scenario, and a movie theater scenario. The experimental results show that SonarBeat can achieve a low mean estimation error for breathing rate estimation, with a medium error of 0.2 bpm. we also find that SonarBeat is highly robust to different experimental parameters and settings.

The main contributions of this paper include the follows.

- Through an analysis and experiments, we validate the feasibility of leveraging active the sonar phase information for breathing rate estimation. To the best of our knowledge, this is the first work to employ active sonar phase information for breathing monitoring with smartphones.
- We design the SonarBeat system based on the analysis and address the technical challenges on using active sonar phase. We implement several signal processing algorithms, including signal generation, data extraction, received signal preprocessing, and breathing rate estimation. Specially, we propose an adaptive median filter approach for removing the static vector in the received signal, which allows to effectively extract the inaudible phase information.
- We prototype the SonarBeat system with two different smartphones, i.e., a Samsung Galaxy S6 and a Samsung Galaxy S7 Edge, and validate its superior performance by comparison with an existing scheme in three different indoor scenarios. Our experimental results demonstrate the superior performance of SonarBeat under different environment factors and different experimental parameters.

In the remainder of this paper, we present the sonar phase analysis in Section II and present the SonarBeat design in Section III. We validate its performance in Section IV. Section V summaries this paper.

II. Sonar Phase Analysis

We propose to use smartphones to monitor vital signs by utilizing an inaudible sound signal, where the speaker and microphone of the smartphone emulates an active sonar system. In particular, the speaker transmits an inaudible sound signal in the frequency range of 18–22 kHz, in the form of a CW signal as $C(t) = A\cos(2\pi ft)$, where A is the amplitude and f is the frequency of the sound. Then the signal is reflected by the chest of the person and is then received by the microphone at a sampling rate of 48 kHz. Because the speaker and microphone use the same frequency, there is no carrier frequency offset (CFO) errors between the sender and receiver. Thus, we can exploit the phase of the inaudible signal data at the receiver to estimate the vital sign. The recent works [17], [18] use the phase of OFDM and CW sonar for finger tracking, while this paper is focused on exploiting CW waves for respiration monitoring.

To obtain the phase of the CW wave, we need to design a coherent detector structure in the receiver to down-convert the received sound signal to a baseband signal. The SonarBeat design is to first split the received sound signal into two identical copies. Then, these two copies are multiplied with the transmitted signal $C(t) = A\cos(2\pi ft)$ and its phase shifted version $C'(t) = -A\sin(2\pi ft)$. Finally, the corresponding In-phase and Quadrature signals are obtained by using a low-pass filter to remove the high frequency components.

We first present a simple analysis for the ideal case that there is no multipath effect (or, for the high signal-to-noise (SNR) regime, where the line-of-sight (LOS) component is the dominant part of the received signal). Under the assumption, the inaudible signal travels through a single path (i.e., from the speaker to the chest, and then from the chest to the microphone) and the propagation delay can be modeled as $d(t) = (D_0 + D\cos(2\pi f_b t))/c$, where D_0 is the constant distance of the path, D and f_b are the amplitude and frequency of the chest movements caused by breathing, respectively, and c is the speed of the sound. The received inaudible signal from this path can be modeled as $R(t) = A_r\cos\left(2\pi ft - 2\pi fd(t) - \theta\right)$, where A_r is the amplitude of the received inaudible signal and θ is a constant phase offset due to the delay in audio recording and playing. To estimate the phase of the inaudible signal, we need to remove the high frequency components. Multiplying the received signal with $C(t) = A\cos(2\pi ft)$, we have

$$\begin{aligned} &A_r\cos(2\pi ft - 2\pi fd(t) - \theta) \times A\cos(2\pi ft) \qquad (1)\\ &= \frac{A_r A}{2}(\cos\left(4\pi ft - 2\pi fd(t) - \theta\right) + \cos(-2\pi fd(t) - \theta)). \end{aligned}$$

The first term in (1) has a high frequency of $2f$, which can be removed with a properly designed low-pass filter. Thus, the I-component of the baseband is extracted as $I = \frac{A_r A}{2}\cos\left(-2\pi fd(t) - \theta\right)$. With a similar approach (i.e., multiplying by $C'(t)$ and removing the high frequency component), we can estimate the Q-component of the baseband signal as $Q = \frac{A_r A}{2}\sin\left(-2\pi fd(t) - \theta\right)$. We then demodulate the phase of the inaudible signal data as

$$\begin{aligned} \varphi(t) &= \arctan(Q/I) = -2\pi fd(t) - \theta \\ &= -2\pi f(D_0 + D\cos(2\pi f_b t))/c - \theta. \qquad (2) \end{aligned}$$

The phase of the inaudible signal, $\varphi(t)$, is a periodic signal with the same frequency as the breathing signal, under this single person scenario with only one propagation path. So the breathing rate f_b can be estimated from (2).

In reality, the received inaudible signal is a complex signal, as a sum of multiple reflected signals (e.g., on the chest as

well as on other surfaces) and interference signals from other sources. In the signal space, we can lump all the other signals into a static vector component rooted at the origin, while the desired signal is a smaller dynamic vector adding to the tip of the static vector. If there is no movements in the neighborhood, the static vector will be relatively constant, while the dynamic vector oscillates on the tip of the static vector following chest movements (see [1] and the extended journal version). To accurately monitor the breathing beats under a multipath and noisy environment, we need to remove the static vector and demodulate the phase information from the dynamic vector. In the following section, we show how to achieve this goal and introduce the design of the SonarBeat system in detail.

III. The SonarBeat System

A. SonarBeat System Architecture

We design the SonarBeat system for tracking breathing beats of one person using active sonar phase data. Specifically, the SonarBeat system employs sonar phase data to monitor the periodic signal caused by the rises and falls of the chest when inhaling and exhaling. According to the sonar phase analysis, SonarBeat can effectively exploit the sonar phase information to monitor breathing signals for three reasons. First, the phase information can track the periodic signal of breathing beats with a high accuracy. Moreover, the phase information is sensitive to the small chest movements caused by breathing. Second, compared with other traditional methods, such as Doppler shift and FMCW [10], the phase based approach has a lower latency and complexity. Finally, the sonar phase data is robust to different orientations, different distances, different cloth thickness, and different breathing rates of different persons. It is also robust large movements of the body, which only leads to a change of the stationary component of the phase data, and can be effectively removed by the proposed adaptive median filter method.

Fig. 1 presents the SonarBeat system architecture. It includes four basic modules: (i) Signal Generation, (ii) Data Extraction, (iii) Received Signal Preprocessing, and (iv) Breathing Rate Estimation. The Signal Generation module mainly implements a Pulse-code Modulation (PCM) of the inaudible signal, where a CW inaudible signal at 18 kHz to 22 kHz is generated and modulated with the PCM technique. The Data Extraction module is to detect the audio signal, which employs a short-time Fourier transform (STFT) based method for audio signal detection. Then, a threshold based method is proposed for detecting the beginning part of the received inaudible signal.

The Received Signal Preprocessing module consists of I/Q demodulation, static vector effect reduction, phase extraction, and data calibration. For I/Q demodulation, we first reduce the sampling rate from 48 kHz to 480 Hz, which can achieve a lower processing delay for realtime monitoring. Then, a coherent detector structure is used to down-convert the received signal to a baseband signal, while a low-pass filter is used to remove the high-frequency components and environment noises to obtain the In-phase and Quadrature components. For

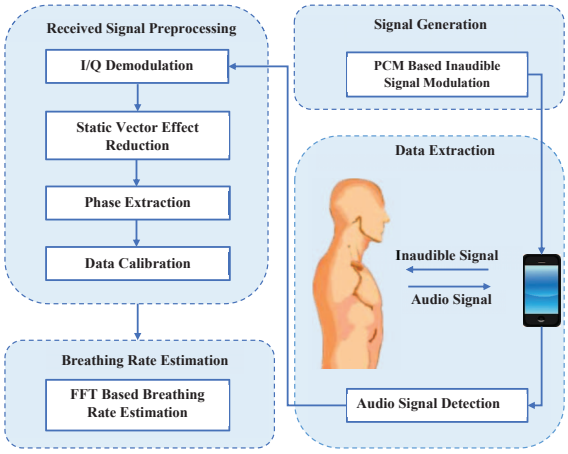

Fig. 1. SonarBeat system architecture.

static vector effect reduction reduction, we propose an adaptive median filter method to remove the static vector of the In-phase and Quadrature signals, which is suitable for realtime processing. For phase extraction, we derive the sonar phase information, which includes the breathing signal. Moreover, we need to unwrap the phase data to obtain the calibrated breathing phase result. For data calibration, we implement a median filter as a simple Low Pass FIR to remove the noises. The Breathing Rate Estimation module employs an FFT based method to estimate the breathing rate.

In the remainder of this section, we discuss the four modules of SonarBeat in detail.

B. Signal Generation

The signal generation module uses one speaker of the smartphone as transmitter, to produce the inaudible signals for breathing monitoring. We implement the signal generation module as a PCM based inaudible signal modulation on the Android platform.

Specifically, the speaker generates an inaudible sound signal in the frequency range of 18–22 kHz in the form of a CW signal $C(t) = A\cos(2\pi ft)$. We produce the sampled analogy signal and then use the PCM technique to digitally represent the sampled CW signal. To generate a PCM stream, the amplitude of the analog CW signal is sampled at uniform intervals, where each sampled value is quantized. The PCM based inaudible signal modulation is implemented with the AudioTrack class.

C. Data Extraction

We use the microphone of the smartphone with a sampling rate of 48 kHz to receive the inaudible signal reflected from the chest of the person. In fact, the microphone is likely to record other sound signals with different frequencies from the surrounding environment. We implement an audio signal detection method to identify the beginning of the inaudible signal from the speaker as follows.

We propose an STFT based method for audio signal detection. When the microphone receives the beginning of inaudible

signal, there will be a large change of power at the inaudible carrier frequency. A threshold based method is proposed for detecting the beginning of the inaudible signal. We adopt a window size of 512 points for estimating the spectrum in STFT. Moreover, we set a threshold of 200 for the power change to detect the beginning of the inaudible signal. In fact, if we detect the power change with the threshold method, the beginning of the inaudible signal can be set as the ending location of the STFT chirp.

D. Received Signal Preprocessing

The Received Signal Preprocessing module consists of four components, including I/Q Demudulation, Static Vector Effect Reduction, Phase Extraction, and Data Calibration. We discuss the design of these components in the following.

1) I/Q Demodulation: Before I/Q Demodulation, we need to down-sample the received signal $R(t) = A_r \cos(2\pi f t - 2\pi f d(t) - \theta)$ for reducing the computation complexity, which is necessary for realtime breathing monitoring. The original system sampling frequency of 48 kHz is reduce to 480 Hz with a down-sampling ratio of 100. Then, we implement the I/Q demodulation to get the I-component and Q-component of the baseband signal using the coherent detector structure. The design is to split the received audio signal into two identical copies. Due to the down-sampling ratio of 100, these two copies should be multiplied with the signal $A\cos(2\pi\frac{f}{100}t)$ and its phase shifted version $-A\sin(2\pi\frac{f}{100}t)$ to obtain the I-component and Q-component of the baseband signal. Because we use phase modulation for breathing monitoring, down-sampling only reduce the number of samples of the amplitude of breathing signal, rather than the phase information.

Finally, a low-pass filter is employed to obtain the corresponding In-phase and Quadrature signals. The low-pass filter has a cutoff parameter of 1 Hz, a sampling rate of 480 Hz, and a resonance of 2. This setting has been shown to be effective for removing the high frequency components and environment audible noises. From Figs. 2 and 3, we can see the raw I-component and Q-component of the baseband signal after the low-pass filters (the dashed curves), which, however, still include their static vectors.

2) Static Vector Effect Reduction: As discussed, the performance of SonarBeat on breathing estimation largely depends on mitigating the effect of the static vector in multipath environments. This is because usually the static vector is much stronger than the dynamic vector that representing the small chest movements. It is difficult to detect the weak breathing signal if we directly use the received sound signal without removing the static vector. Recently, there are two methods proposed for static vector effect reduction. The Dual-Differential Background Removal approach is used for hand tracking with 60 GHz millimeter wave (mmWave) signals [19]. The method is susceptible to environment noise and long latency, which is not effective for breathing monitoring. The second scheme, Local Extreme Value Detection (LEVD) [17], is used to track hand movement. The method requires an

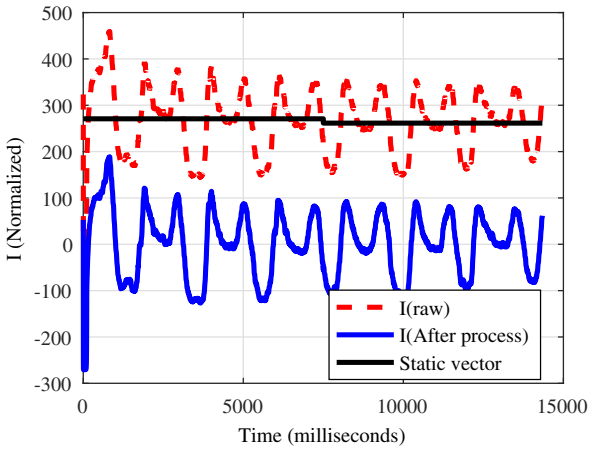

Fig. 2. The adaptive filter median for removing the static vector in the baseband component I.

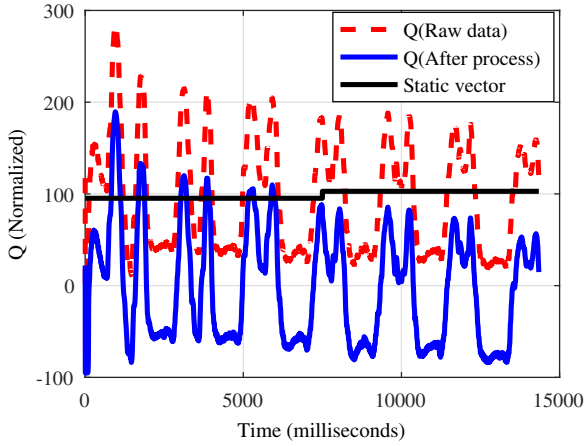

Fig. 3. The adaptive filter median for removing the static vector for the baseband component Q.

empirical threshold for detecting the stationary vector, which is not robust for different environments and different persons.

In Algorithm 1, we present an adaptive median filter method for removing the static vector, which has a low latency and is robust for different environments. The idea is to use a window to obtain the median for estimating the static vector. The only parameter is the window size w, which is robust for different environments. For one baseband signal component $I(n)$ or $Q(n)$, for $n = 0, 1, ..., N-1$, we partition it into multiple non-overlapping sublists (each is denoted by $W[1, 2, ..., w]$) with a window size w and a single sublist $R[1, 2, ..., r]$ with a window size r, where r is the number of remaining elements of $I(n)$ or $Q(n)$ not included in the previous W sublists. The sublists $W[1, 2, ..., w]$ and sublist $R[1, 2, ..., r]$ are used to estimate the medians for the first $n_w - 1$ windows and the last window, respectively, where $n_w = \lfloor N/w \rfloor$. Finally, the output $O(n)$, for $n = 0, 1, ..., N-1$, can be obtained as in Steps 14 and 21 by removing the static vector. The proposed method is simple and robust for realtime processing of received data in different environments with a low delay.

Fig. 2 and Fig. 3 show the adaptive median filter method for removing the static vectors in the baseband signal components

Algorithm 1: The Adaptive Median Filter Method

Input: One baseband signal component: $X(n) = I(n)$ or $Q(n)$ for $n = 0, 1, ..., N-1$ and the window size w ;
Output: Real or Imaginary part after removing the static vector: $O(n)$ for $n = 0, 1, ..., N-1$;
//Initialize ;
n_w: Number of windows;
r: Number of the remaining elements of $X(n)$, which cannot form a full W window;
$W[1, 2, ..., w]$: Sublists with window size w;
$R[1, 2, ..., r]$: Sublist with the remaining r elements;
//Find the median for each window;
for $i = 0 : n_w$ **do**
  if $((i+1) * w) <= N$ **then**
    $W[1, 2, ..., w] \leftarrow X((w * i)$ to $((i+1) * w - 1))$;
    $M \leftarrow$ the median of $W[1, 2, ..., w]$,;
    for $j = w * i : (i+1) * w$ **do**
      $O(j) = X(j) - M$;
    end
  end
  else if $r! = 0$ **then**
    $R[1, 2, ..., r] \leftarrow X((w * i)$ to $(w * i + r - 1))$;
    $M \leftarrow$ the median of $R[1, 2, ..., r]$;
    for $j = w * i : (i+1) * w$ **do**
      $O(j) = R(j) - M$;
    end
  end
end
Return $O(n)$ for $n = 0, 2, ..., N-1$;

I and Q, respectively. We can see that the estimated static vector data can represent well the average amplitude information for the baseband signal components. After the adaptive median filter, the components I and Q are roughly centered at zero, making it easier for extracting the breathing signal they carry.

3) Phase Extraction: After removing the static vector based on the adaptive median filter method, we can extract the phase data in the I-Q plane, which only includes the dynamic breathing component. Let $O_I(t)$ and $O_Q(t)$ denote the output values of Algorithm 1 after removing static vectors for the corresponding I and Q data, respectively. The phase for the inaudible signal can be computed with (2), that is

$$\varphi(t) = \arctan\left(\frac{O_Q(t)}{O_I(t)}\right). \tag{3}$$

With (2) and (3), we find the phase values $\varphi(t)$ for the breathing signals reflected from the chest. Although the reflected breathing signal may still have multipath components, these multipath signals have the same breathing frequency but with different phase shifts, each of which is a constant. Thus, the breathing rate is not affected by the dynamic multipath effect. This is different from hand tracking, which requires only one path from the smartphone and the hand. Thus, our SonarBeat can estimate the breathing rate using a single subcarrier rather than multiple subcarriers. Fig. 4 presents the respiration curve obtained from the phase data with its static vectors removed. It is noticed that the magnitude of the breathing signal is large, which is periodic if we can remove

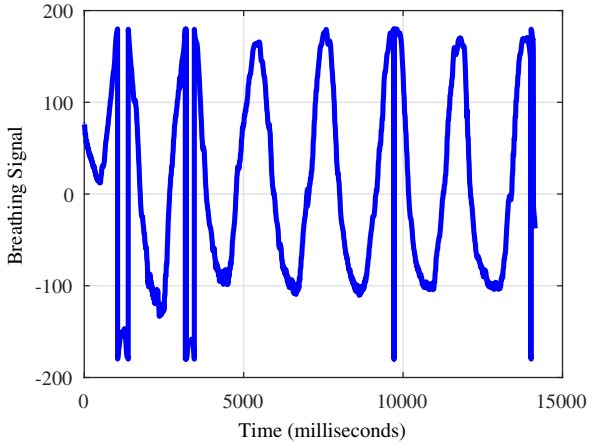

Fig. 4. Respiration curve obtained from the phase data with the static vector effect removed.

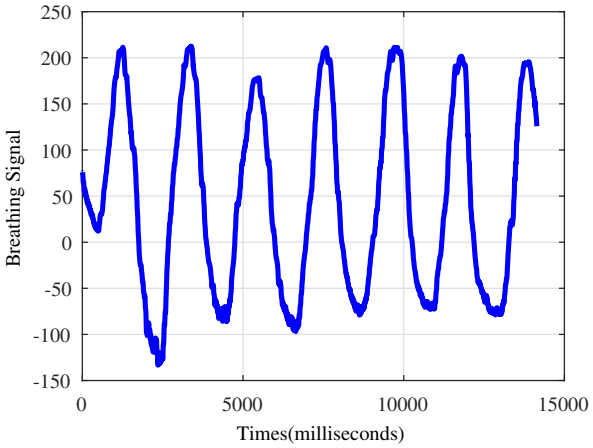

Fig. 5. Respiration curve for phase data after unwrapping the phase data.

the sudden phase changes. Thus, we need to implement a data calibration scheme for the demodulated phase data to achieve a better accuracy.

4) Data Calibration: For data calibration, we implement a phase unwrapping scheme for recovering the right phase values, as well as a median filter for reducing the environment noise. To estimate breathing rates, we need to obtain the right breathing curve for phase data. Because the phase value will have a change of 2 π for every wavelength distance, we implement the phase unwrapping to process the demodulated phase data to obtain the right breathing curve. Fig. 5 shows the respiration curve obtained from the phase data after phase unwrapping. It is a clean breathing signal with smaller environment noises. On the other hand, we adopt the median filter method for removing environment noise, where the filter window size is set to 300. Fig. 6 presents the respiration curve for unwrapped phase data after the median filter, which is useful for accurate breathing rate estimation.

E. Breathing Rate Estimation

SonarBeat has three stages for breathing monitoring by using the calibrated inaudible phase data. In the first stage of a 15-second duration, we cannot effectively estimate the

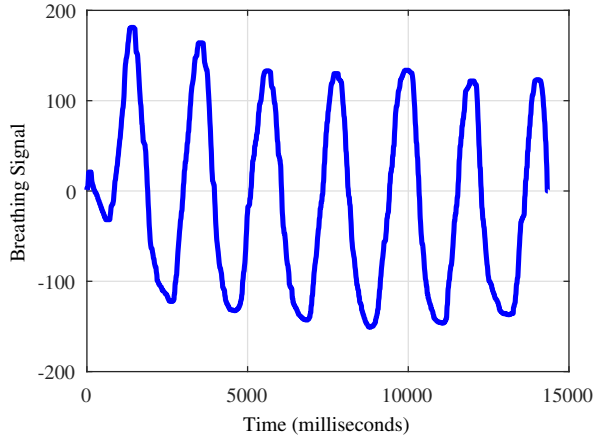

Fig. 6. Respiration curve for unwrapped phase data after the median filter.

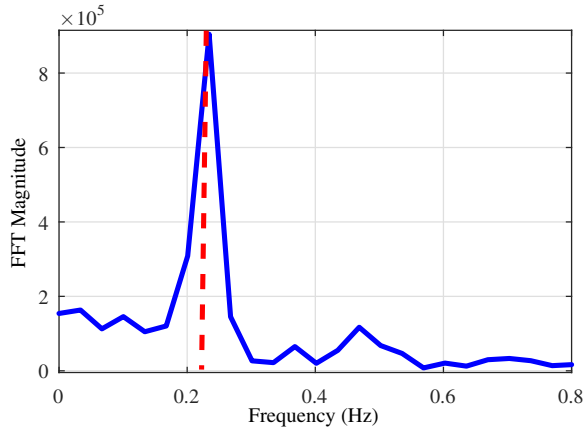

Fig. 7. Respiration rate estimation based on FFT.

breathing rate, because the phase data in a window can continually change when new data arrive. In the second stage, we exploit the 15-second phase data to estimate the breathing rate in realtime with the FFT based method. In fact, the frequency resolution depends on the window size of FFT. If the window size becomes larger, the estimation accuracy will be higher, but the larger window size also leads to a lower time domain resolution. Thus, for online breathing rate estimation, we use the same window size, which is in fact equal to that of the STFT based method. It balances the tradeoff between the frequency domain resolution and the time domain resolution. In the final stage, we use all the phase data from the three stages for breathing beats estimation with the FFT based method, which can achieve a higher estimation accuracy. Fig. 7 illustrates the FFT based respiration rate estimation. We can see that the estimated frequency for breathing beats of a single person is 0.23 Hz, which is approximately the same as the true breathing rate measured by the NEULOG Respiration Monitor Belt Logger Sensor.

IV. Experimental Study

A. Implementation and Test Configuration

We prototype the SonarBeat system with two different smartphones, a Samsung Galaxy S6 and a Samsung Galaxy S7 Edge, both of which are based on the Android platform. Moreover, we implement all the signal processing algorithms in Java using the Android SDK. Both smartphones perform well on processing the audio data for realtime breathing rate monitoring and display. The first edition of SonarBeat is implemented with the minimum version of Android 5.1.1 OS (API 21). So it works with all the more recent Andriod systems such as Android 6.0 and Android 7.0. For breathing monitoring, we only use one speaker and one microphone to transmit and receive the inaudible audio data, while the microphone and speaker are fixed at the bottom on the smartphone. Furthermore, we use the AudioTrack class to play inaudible sound and the AudioRecord class to record sound. The buffer of the recording thread is set to 1920 points with a sampling rate of 48 kHz. Therefore, we set the realtime signal processing unit to 1920 points, which is about 40ms.

We conduct extensive experiments with SonarBeat with five persons over three months. The test scenarios include an office, a bedroom and a movie theater. The *office* is a 4.5×8.8 m^2 room. The room is crowed with tables and PCs, which form a complex propagation environment. In this office environment, we measure breathing monitoring data under different system parameters. The second environment is a *bedroom* of 3.9×6 m^2, where we test breathing monitoring for a single person. The third setup is a *movie theater* of a large 27×40 m^2 area, where many people are watching a movie, and there are audio interferences from the movie and other people. For comparison purpose, we use the NEULOG Respiration Monitor Belt Logger Sensor to record the ground truths of the breathing rates.

B. Performance of Breathing Rate Estimation

Fig. 8 presents the cumulative distribution functions (CDF) of estimation error in breathing rate estimation with SonarBeat. For comparison purpose, we also developed an LEVD based system [17], where the LEVD method is used for estimating the static vector and all other signal processing methods are the same as in SonarBeat. The LEVD based system is used as a benchmark in the experiment. We find that SonarBeat and the LEVD based method achieve a median error of 0.2 bpm and 0.3 bpm, respectively. This illustrates that both systems can effectively estimate breathing rates. However, it is worth noting that for SonarBeat, 95% of the test results have an estimated error under 0.5 bpm, while only 60% of the test results with the LEVD based method have an estimated error under 0.5 bpm. Moreover, the maximum estimation error for SonarBeat and the LEVD based method are 2.4 bpm and 5 bpm, respectively. This is because the LEVD based method requires setting the empirical threshold based on the standard deviation of the baseband signal in a static environment. It is not robust in varying environments where the same threshold will not work. However, SonarBeat leverages the adaptive median filter method, and is thus more robust to changes in the environment. Therefore, the SonarBeat system can achieve a higher and more stable breathing rate estimation accuracy than the LEVD based method.

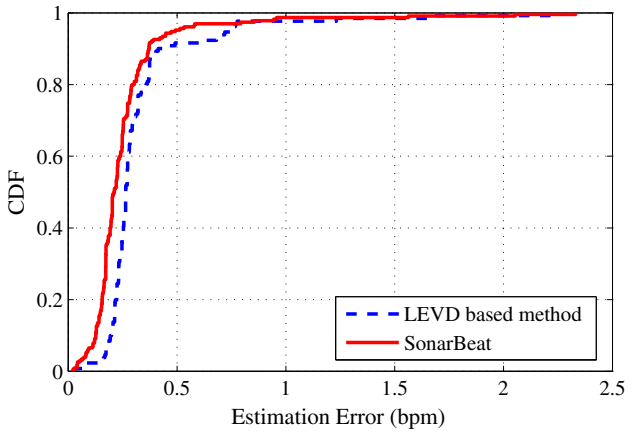

Fig. 8. CDFs of estimation error in breathing rate estimation.

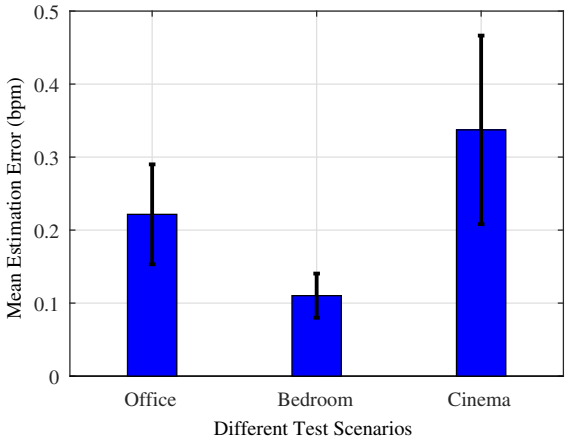

Fig. 9. Mean estimation error for three different scenarios.

Fig. 9 presents the mean estimation errors for the three different scenarios, which are 0.22 bpm, 0.11 bpm, and 0.33 bpm for the office, bedroom and cinema scenarios, respectively. We plot the 95% confidence intervals as error bars. It is noticed that the mean estimation error for the bedroom case is the minimum, because the bedroom has a better environment: with smaller noise and no sound interferences from other persons. This shows that SonarBeat is suitable for breathing monitoring during sleeping, which effectively detects apnea or abnormal breathing. For breathing monitoring in the office, the performance is worse than the bedroom. This because there is a more complex propagation environment and interferences from other people. Furthermore, large noises from computers, air conditioners, and other equipment also influences the inaudible signal. For breathing monitoring in the cinema, we find that it has the largest mean estimation error and variance because of the more complex environment and stronger noises. In fact, breathing monitoring in the cinema is still quite accurate given the extremely adverse environment. These experiments validate that SonarBeat system is highly accurate and robust in different scenarios.

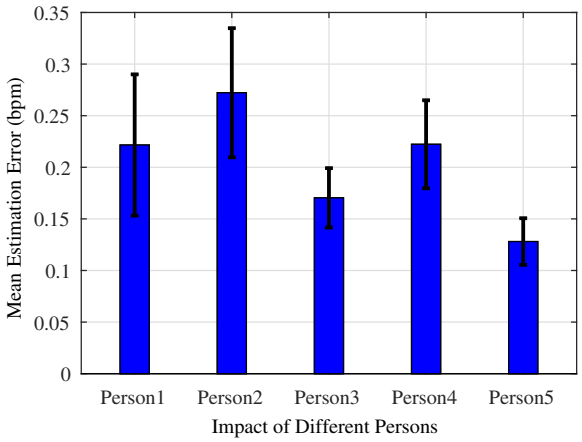

Fig. 10. Impact of different test persons.

C. Impact of Various Test Factors

Fig. 10 shows the impact of different persons in the office scenario. In the experiment, we test five persons including three men and two women, respectively, where every volunteer wears the NEULOG Respiration unit for recording the benchmark result for breathing data. From Fig. 10, we can see that Person 3, Person 4, and Person 5 have a lower mean estimation error. This is because they work out quite often and have a strong respiration, leading to stronger breathing signals. On the other hand, the other two persons have weaker breathing magnitudes, but their estimation errors are still under 0.5 bpm, which is acceptable. Thus, we can see that SonarBeat is adaptive for different persons.

Fig. 11 shows the impact of different distances between the chest and the smartphone. When the distance is increased, the accuracy for breathing estimation become lower. Particularly, we can see that for a distance of 55 cm, the mean breathing estimation error becomes 1 bpm with a larger variance. In this experiment, we find that ultrasound wave at 18 kHz to 22 kHz experiences a large attenuation, and the microphone will receive a lower power from the reflection of the chest movements if the distance is increased. Moreover, breathing rate estimation with SonarBeat depends on I/Q demodulation. The magnitude of the I/Q components becomes weaker when the distance is increased, leading to higher errors. To improve the measurement distance, we leverage the parameter resonance of the low-pass filter to strengthen the amplitude of the inaudible signal near the cutoff frequency, thus improving the magnitudes of I/Q components. In the experiment, we set the cutoff frequency to 40 Hz for the sampling rate of 48 kHz. We can see that under 50 cm, the proposed system can achieve very good accuracy.

Fig. 12 shows the impact of chest orientation relative to the smartphone in the office scenario, where we consider three cases including 0^{circ}, 45^{circ} and 90^{circ}. It is noticed that at 0^{circ} direction with the front orientation relative to the smartphone, we can obtain the minimum mean estimation error at about 0.22 bpm. Moreover, at the 90^{circ} direction, the maximum mean estimation error of 0.39 bpm is achieved. The

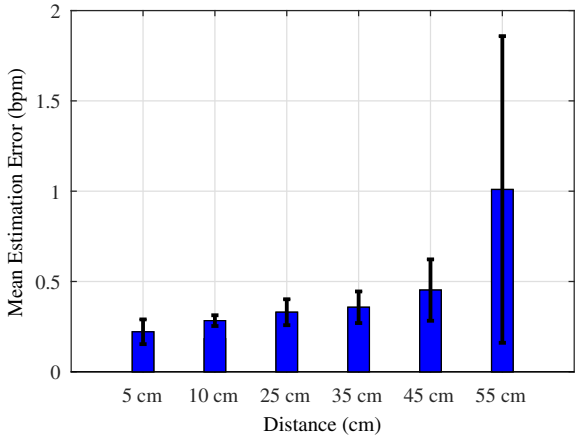

Fig. 11. Impact of the distance between the chest and the smartphone.

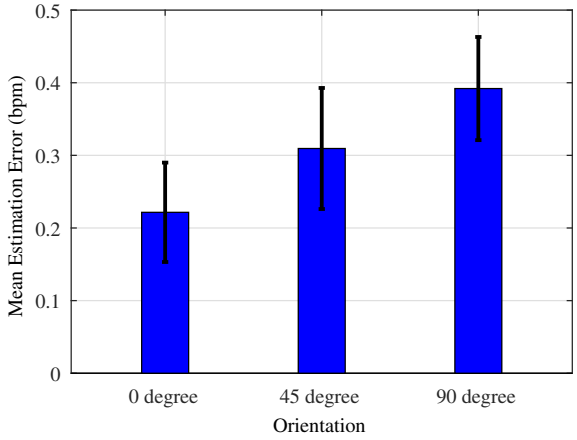

Fig. 12. Impact of chest orientation relative to the smartphone.

reason is that the received inaudible signal is the strongest when the person faces the smartphone speaker. It is most effective on monitoring the breathing signal for the chest movements in this scase. Thus, we can obtain the higher estimation accuracy at the front direction.

V. Conclusions

In this paper, we presented SonarBeat, a smartphone based system that exploits phase based sonar to monitor breathing beats. We first provided a sonar phase analysis and proved that the sonar phase based method can extract breathing signals. We then described the SonarBeat design in detail, including its signal generation, data extraction, received signal preprocessing, and breathing rate estimation modules. Finally, we implemented SonarBeat with two different smartphones, and conducted an extensive experimental study with three test scenarios. The experimental results validated that SonarBeat can achieve superior performance on breathing beats estimation under different environments. A demo of the SonarBeat system will be presented [20].

Acknowledgment

This work is supported in part by the US National Science Foundation (NSF) under Grant CNS-1702957, and through the Wireless Engineering Research and Education Center (WEREC) at Auburn University. Any opinions, findings, and conclusions or recommendations expressed in this material are those of the authors and do not necessarily reflect the views of the foundation.

References

[1] X. Wang, C. Yang, and S. Mao, "PhaseBeat: Exploiting CSI phase data for vital sign monitoring with commodity WiFi devices," in *Proc. IEEE ICDCS 2017*, Atlanta, GA, June 2017, pp. 1–10.

[2] ——, "Tensorbeat: Tensor decomposition for monitoring multi-person breathing beats with commodity WiFi," *ACM Transactions on Intelligent Systems and Technology*, 2017.

[3] O. Boric-Lubeke and V. Lubecke, "Wireless house calls: Using communications technology for health care and monitoring," *IEEE Microwave Mag.*, vol. 3, no. 3, pp. 43–48, Apr. 2002.

[4] C. Hunt and F. Hauck, "Sudden infant death syndrome," *Can. Med. Assoc. J*, vol. 174, no. 13, pp. 1309–1310, Apr. 2006.

[5] N. H. Shariati and E. Zahedi, "Comparison of selected parametric models for analysis of the photoplethysmographic signal," in *Proc. 1st IEEE Conf. Comput., Commun. Signal Process.*, Kuala Lumpur, Malaysia, Nov. 2005, pp. 169–172.

[6] M. L. R. Mogue and B. Rantala, "Capnometers," *Journal of clinical monitoring*, vol. 4, no. 2, pp. 115–121, Apr. 1988.

[7] A. Droitcour, O. Boric-Lubecke, and G. Kovacs, "Signal-to-noise ratio in Doppler radar system for heart and respiratory rate measurements," *IEEE Trans. Microw. Theory Technol.*, vol. 57, no. 10, pp. 2498–2507, Oct. 2009.

[8] P. Nguyen, X. Zhang, A. Halbower, and T. Vu, "Continuous and fine-grained breathing volume monitoring from afar using wireless signals," in *Proc. IEEE INFOCOM'16*, San Francisco, CA, Apr. 2016, pp. 1–9.

[9] J. Salmi and A. F. Molisch, "Propagation parameter estimation, modeling and measurements for ultrawideband mimo radar," *IEEE Trans. Microw. Theory Technol.*, vol. 59, no. 11, pp. 4257–4267, Nov. 2011.

[10] F. Adib, H. Mao, Z. Kabelac, D. Katabi, and R. Miller, "Smart homes that monitor breathing and heart rate," in *Proc. ACM CHI'15*, Seoul, Korea, April 2015, pp. 837–846.

[11] H. Abdelnasser, K. A. Harras, and M. Youssef, "Ubibreathe: A ubiquitous non-invasive wifi-based breathing estimator," in *Proc. IEEE MobiHoc'15*, Hangzhou, China, June 2015, pp. 277–286.

[12] Z. Yang, P. Pathak, Y. Zeng, X. Liran, and P. Mohapatra, "Monitoring vital signs using millimeter wave," in *Proc. IEEE MobiHoc'16*, Paderborn, Germany, July 2016, pp. 211–220.

[13] J. Liu, Y. Wang, Y. Chen, J. Yang, X. Chen, and J. Cheng, "Tracking vital signs during sleep leveraging off-the-shelf WiFi," in *Proc. ACM Mobihoc'15*, Hangzhou, China, June 2015, pp. 267–276.

[14] H. Aly and M. Youssef, "Zephyr: Ubiquitous accurate multi-sensor fusion-based respiratory rate estimation using smartphones," in *Proc. IEEE INFOCOM'16*, San Francisco, CA, Apr. 2016, pp. 1–9.

[15] Y. Ren, C. Wang, J. Yang, and Y. Chen, "Fine-grained sleep monitoring: Hearing your breathing with smartphones," in *Proc. IEEE INFOCOM'15*, Hong Kong, China, Apr. 2015, pp. 1194–1202.

[16] R. Nandakumar, S. Gollakota, and N. Watson, "Contactless sleep apnea detection on smartphones," in *Proc. ACM MobiSys'15*. Florence, Italy: ACM, May 2015, pp. 45–57.

[17] W. Wang, A. X. Liu, and K. Sun, "Device-free gesture tracking using acoustic signals," in *Proc. ACM MobiCom'16*. New York City, NY: ACM, Oct. 2016, pp. 82–94.

[18] R. Nandakumar, V. Iyer, D. Tan, and S. Gollakota, "Fingerio: Using active sonar for fine-grained finger tracking," in *Proc. ACM CHI'16*. Santa Clara, CA: ACM, June 2016, pp. 1515–1525.

[19] T. Wei and X. Zhang, "mTrack: High-precision passive tracking using millimeter wave radios," in *Proc. ACM Mobicom'15*. Paris, France: ACM, Sept. 2015, pp. 117–129.

[20] X. Wang, R. Huang, and S. Mao, "Demo abstract: SonarBeat: Sonar phase for breathing beat monitoring with smartphones," in *Proc. IEEE SECON 2017*, San Diego, CA, June 2017.